Title: Crystal structure, infrared spectra and microwave dielectric properties of novel extra low-temperature fired $Eu_2Zr_3(MoO_4)_9$ ceramics

Authors: Y.H. Zhang, J.J. Sun, N. Dai, Z.C. Wu, H.T. Wu, C.H. Yang

PII: S0955-2219(18)30759-3
DOI: https://doi.org/10.1016/j.jeurceramsoc.2018.12.042
Reference: JECS 12247

To appear in: *Journal of the European Ceramic Society*

Received date: 29 June 2018
Revised date: 18 December 2018
Accepted date: 18 December 2018

Please cite this article as: Zhang YH, Sun JJ, Dai N, Wu ZC, Wu HT, Yang CH, Crystal structure, infrared spectra and microwave dielectric properties of novel extra low-temperature fired $Eu_2Zr_3(MoO_4)_9$ ceramics, *Journal of the European Ceramic Society* (2018), https://doi.org/10.1016/j.jeurceramsoc.2018.12.042

Crystal structure, infrared spectra and microwave dielectric properties of novel extra low-temperature fired $Eu_2Zr_3(MoO_4)_9$ ceramics

Y.H. Zhang, J.J. Sun, N. Dai, Z.C. Wu, H.T. Wu*,C.H.Yang*

School of Materials Science and Engineering, University of Jinan, Jinan 250022, China

Abstract

A new kind of low-temperature fired $Eu_2Zr_3(MoO_4)_9$ ceramic was fabricated by conventional solid-state reaction method. The mixed powders was calcined at 600 ℃ and the samples were sintered at 500 ℃ to 700 ℃ for 4h. X-ray diffraction analysis and Rietveld refinement indicated that $Eu_2Zr_3(MoO_4)_9$ belonged to a trigonal system with space group R-3c. Bond ionicity, lattice energy and bond energy of the ceramic were calculated by the complex chemical bond theory. Microwave dielectric properties were determined at microwave frequencies of 9.7-14.7 GHz by a network analyzer. Far infrared spectra indicated the main contribution to polarization for $Eu_2Zr_3(MoO_4)_9$ ceramics was the absorption of structural phonon oscillation. The ceramic sintered at 600 ℃ for 4h exhibited the best dielectric properties with a relative permittivity (ε_r) of 10.75, a quality factor ($Q{\cdot}f$) of 74,900 GHz and a temperature coefficient of resonance frequency (τ_f) of -8.88 ppm/℃.

Keywords: Microwave dielectric properties; $Eu_2Zr_3(MoO_4)_9$; Low-temperature sintering; Far infrared spectra

1. Introduction

With the rapid development of wireless communication technology, microwave dielectric ceramics has been widely used in many fields such as mobile communications and radar systems [1]. Microwave dielectric ceramics should possess an appropriate relative permittivity, a higher quality factor and a near-zero temperature coefficient of the resonant frequency [2, 3]. A series of dielectric ceramics with excellent microwave dielectric properties were reported in the past. [4-9] Some typical microwave dielectric ceramics such as Al_2O_3-TiO_2 [10, 11] and complex perovskites (ABB'O_3) [12] possess excellent microwave dielectric properties, however, their applications in highly intergrated circuits are limited due to the high sintering temperature.Usually, in order to reduce the sintering temperature, sintering additives such as fluoride and CuO addition were often used. [13, 14] In the past few decades, numerous glass-free low firing ceramics have been investigated, such as $BaMg_2V_2O_8$ and $Ba_2LnV_3O_{11}$ (Ln=Nd, Sm) [15, 16]. In the recent years, some new ceramic systems as well as low temperature fired ceramics have been reported [17-24]. For example, $Li_9Zr_3NbO_{13}$ sintered at 900 ℃ exhibited the excellent microwave dielectric properties of ε_r=21.3, $Q{\cdot}f$=43,600 GHz and τ_f=7.3 ppm/℃ [23], (1-x)Li_2TiO_3-xLi_2CeO_3 ceramic could be densified at 850 ℃ and possessed microwave dielectric properties of ε_r=21.2, $Q{\cdot}f$=59,039 GHz and τ_f=-7.4 ppm/℃ when x=0.14 [24].

Molybdenum (Mo) containing microwave dielectric ceramics has been widely studied due to its low sintering temperature and superior microwave dielectric performances [25-27]. Pang et al. reported that $CaMoO_4$-xY_2O_3-xLi_2O system possessed good microwave dielectric properties with ε_r=9.5, $Q{\cdot}f$=63,240 GHz and τ_f=7.2 ppm/℃ when x=0.306 and sintered at 775 ℃ [25]. Pang et al. also investigated the microwave dielectric properties of $Ln_2Mo_3O_{12}$ (Ln=La, Nd) ceramics. $La_2Mo_3O_{12}$ sintered at 930 ℃ exhibited a low ε_r of 10.1, a high $Q{\cdot}f$ of 60,000 GHz and a τ_f of -80 ppm/℃ and $Nd_2Mo_3O_{12}$ sintered at 945 ℃ exhibited a ε_r of 8.2, a high $Q{\cdot}f$ of 80,000 GHz and a τ_f of -60 ppm/℃ [26]. Furthermore, Zhang et al. [27] reported two ultra-low temperature sintered microwave dielectric ceramics $Ag_2Mo_2O_7$ and $Ag_6Mo_{10}O_{33}$. The former had an excellent properties with ε_r=13.3, $Q{\cdot}f$=25,300 GHz and τ_f=-142 ppm/℃ when sintered at 460℃ and the latter with ε_r=14, $Q{\cdot}f$=8,500 GHz and τ_f=-50 ppm/℃ when sintered at 500 ℃.

Recently, Liu et al. [28] reported $Ln_2Zr_3(MoO_4)_9$ (Ln=Sm, Nd) ceramics exhibited good microwave dielectric properties when samples sintered at 875 ℃ and 850℃, respectively. Subsequently, Liu et al. [29] reported that $La_2Zr_3(MoO_4)_9$ ceramics sintered at 775 ℃ for 4 h possessed excellent microwave dielectric properties of ε_r=10.8, $Q{\cdot}f$=50,628 GHz and τ_f=-38.8 ppm/℃. On this basis, a new kind of Mo-based $Eu_2Zr_3(MoO_4)_9$ ceramics was investigated in this work and the correlations between microwave dielectric properties and intrinsic factors were studied by the calculation of chemical bond theory and far infrared spectra.

2. Experimental procedure

$Eu_2Zr_3(MoO_4)_9$ ceramics were prepared by solid-state method with a stoichiometric mixture of Eu_2O_3 (99.9 %, Macklin, China), ZrO_2 (99.99 %, Aladdin, China) and MoO_3 (99.9 %, Macklin, China), and the starting chemicals used were all commercially available reagents. The powders were ball-milled in a nylon container with anhydrous ethanol for 24h and then dried and calcined at 600 ℃ in alumina crucible for 2 h to obtain the precursors. Then, the powders were re-milled in the nylon container for 24h. And after being baked in the air dry oven, the precursors mixed with 10 wt% paraffin wax were pressed into cylindrical discs with dimensions of 10 mm in diameter and 6 mm in height. Then, all compacts were heated at 500 ℃ for 4 h to remove the organic binder and the heating rate was 1 ℃/min. Subsequently, the pellets of $Eu_2Zr_3(MoO_4)_9$ were sintered at 500-700 ℃ for 4 h in air.

The crystalline phase composition of the grinding specimens was identified by X-ray diffraction (Model D/MAX-B, Rigaku Co., Japan). Scanning electron microscope (FESEM Quanta 250, FEI Co., America) was used to study the microstructures of the polished and thermally etched surfaces of sintered pellets. The infrared reflectivity spectra were measured by a Bruker IFS 66v FTIR spectrometer on Infrared beamline station (U4). Dielectric behaviors of sintered samples were measured by a network analyzer. Hakki-Coleman dielectric resonator method with the TE_{011} resonant mode was used to measure the relative permittivity and the cavity method with the TE_{01d} mode was used to measure the unloaded quality factors[30, 31]. The temperature coefficients of resonant frequency (τ_f) was measured by the following equation:

$$\tau_f = \frac{f_{85} - f_{25}}{f_{25}(85 - 25)} \times 10^6 \ (ppm \ / ^\circ C) \quad (1)$$

where f_{25} and f_{85} are the TE_{01d} resonant frequency at 25 ℃ and 85 ℃, respectively. The relative density can be achieved through Eq. (2).

$$\rho_{relative} = \frac{\rho_{apparent}}{\rho_{theory}} \times 100\ \% \quad (2)$$

3. Results and discussions

The X-ray diffraction spectrum for calcined powders and $Eu_2Zr_3(MoO_4)_9$ ceramics sintered at 600 ℃ - 700 ℃ were shown in Fig. 1. With different sintering temperatures, the reflections were consistent with each other and they all matched well with the standard pattern of $Eu_2Zr_3(MoO_4)_9$ (JCPDS No. 53-0172). No second phase was detected in the present system. All the samples formed a trigonal structure with space group R-3c and the refinement patterns of $Eu_2Zr_3(MoO_4)_9$ ceramics sintered at 500 ℃ - 700 ℃ were shown in Fig. S1. The final values of lattice parameters, theoretical density and relative density of all samples sintered at various temperatures were listed in Table 1 and the reliability factors were listed in Table S1. Besides, the atomic positions and occupancy of $Eu_2Zr_3(MoO_4)_9$ ceramics sintered at 600 ℃ were shown in Table S2. In addition, the reliability factors of the results were in the range of R_p=4.25 % - 5.29 %, R_{wp}=6.03 %- 6.97 % and χ^2=2.81-5.27, which indicated that the refinement results were credible.

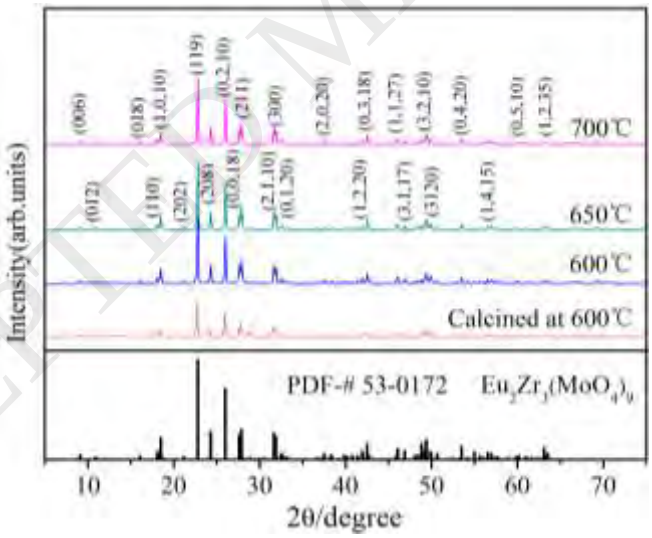

Fig. 1 X-Ray diffraction patterns of calcined powders sintered at 600 ℃ for 2h and $Eu_2Zr_3(MoO_4)_9$ ceramics sintered at 600 ℃-700 ℃ for 4h.

Table 1 The lattice parameters, theoretical densities and relative densities of $Eu_2Zr_3(MoO_4)_9$ ceramics sintered at 500 ℃ - 700 ℃.

S.T. (℃)	$a=b$ (Å)	c (Å)	$\alpha=\beta$ (°)	γ (°)	V (Å^3)	$\rho_{theo.}$ (g/cm^3)	$\rho_{rela.}$ (%)
500	9.787(7)	58.062(8)	90	120	4817.13(1)	4.172(0)	61.40
550	9.784(6)	58.051(5)	90	120	4813.16(5)	4.175(5)	64.15
600	9.786(7)	58.071(1)	90	120	4816.88(0)	4.172(2)	95.10
650	9.785(0)	58.087(6)	90	120	4816.56(4)	4.172(5)	94.82
700	9.786(0)	58.099(3)	90	120	4818.50(2)	4.170(8)	94.71

S.T.— the sintering temperature of $Eu_2Zr_3(MoO_4)_9$ ceramics.

$\rho_{theo.}$— theoretical density of $Eu_2Zr_3(MoO_4)_9$ ceramics.

$\rho_{rela.}$— relative density of $Eu_2Zr_3(MoO_4)_9$ ceramics.

The crystal structure of $Eu_2Zr_3(MoO_4)_9$ ceramics projected on (011) plane was shown in Fig. 2. There were 6 molecules and three types of polyhedron per primitive cell. The Eu atom occupied the 12c Wyckoff position, and the surrounding oxygen atoms formed a tricapped trigonal prism. The two independent zirconium atoms Zr(1) and Zr(2) were coordinated octahedrally with oxygen anions, occupying the 6b and 12c Wyckoff position respectively. The molybdenum atoms had a tetrahedral oxygen environment with Mo(1) lying on the 36f Wyckoff position and Mo(2) lying on the 18e Wyckoff position. Besides, the oxygen anion occupies the 36f Wyckoff position. Simultaneously, MoO_4 tetrahedron, ZrO_6 octahedron and EuO_9 tricapped trigonal prisms linked by their common vertices into an original three-dimensional framework.

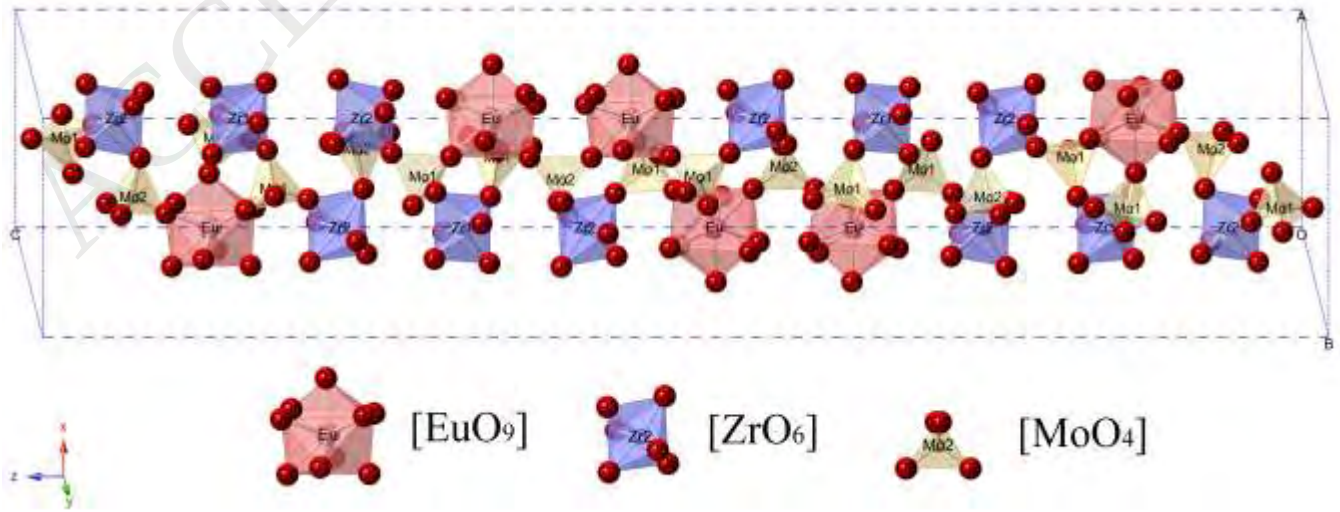

Fig. 2 Schematic representation of the crystal structure for $Eu_2Zr_3(MoO_4)_9$ ceramics.

The relative densities of $Eu_2Zr_3(MoO_4)_9$ ceramics sintered at different temperatures were shown in Table 1. With the increase of sintering temperature, the relative density increased at first and then saturated at 600 ℃ - 700 ℃. Besides, the optimum relative density could reach 95.10 % when the ceramic sintered at 600 ℃. The polished and thermal-etched surfaces of $Eu_2Zr_3(MoO_4)_9$ ceramics sintered at 600 ℃ - 700 ℃ could be observed from Fig. 3 and there were almost no pores exist in the ceramics, which meant that the ceramics were well densified at this temperature range. In addition, with the sintering temperature increases from 600 ℃ to 700 ℃, the grain sizes of samples increased approximately from 0.3 μm to 1 μm.

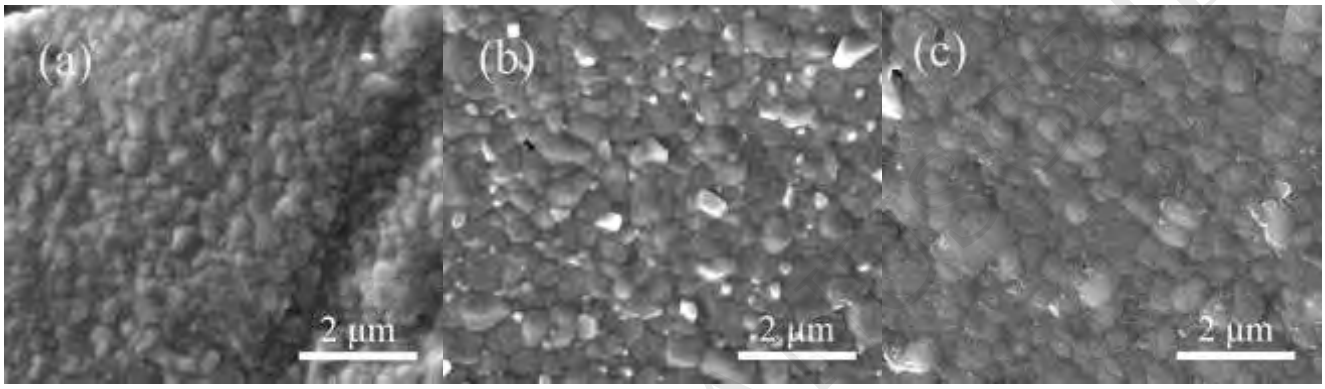

Fig. 3 SEM micrographs of polished and thermal-etched surfaces of $Eu_2Zr_3(MoO_4)_9$ ceramics sintered at different temperatures for 4 h (a-c corresponding to 600 ℃- 700 ℃).

The dielectric properties of $Eu_2Zr_3(MoO_4)_9$ ceramics sintered at 600 ℃ to 700 ℃ was shown in Fig. 4. The tendency of relative permittivity as a function of sintering temperatures was similar with the relative densities of $Eu_2Zr_3(MoO_4)_9$ ceramics, which could be explained by the influence of extrinsic factors on the relative permittivity. When sample sintered at 600 ℃, the relative density reached 95.10 % and the ceramic possessed the best relative permittivity (10.75). Besides, the effect of extrinsic factors on relative permittivity could be ignored when sample sintered at 600 ℃, and the main influence factors were intrinsic factors like polarizability. The theoretical dielectric polarizability ($\alpha_{theo.}$) and observed dielectric polarizability ($\alpha_{obs.}$) were calculated by additive rule reported by Shannon et al. [32] and Clausius-Mossotti equation:

$$\begin{aligned}\alpha_{theo.} &= \alpha(Eu_2Zr_3(MoO_4)_9) \\ &= 2\alpha(Eu^{3+}) + 3\alpha(Zr^{4+}) + 9\alpha(Mo^{6+}) + 36\alpha(O^{2-})\end{aligned} \tag{3}$$

$$\alpha_{obs.} = \frac{1}{b} V_m \frac{\varepsilon - 1}{\varepsilon + 2} \tag{4}$$

where $\alpha(La^{3+})$, $\alpha(Zr^{4+})$, $\alpha(Mo^{6+})$ and $\alpha(O^{2-})$ represent the ions polarizabilities. What's more, b, V_m and ε are constant value ($4\pi/3$), molar volume and relative permittivity of ceramics, respectively. The ion polarizability of Mo^{6+} was calculated by Choi et al. [33] since Shannon did not report the value. In addition, the calculated results $\alpha_{theo.}$=120.61 and $\alpha_{obs.}$=146.56 were roughly approximate and the numerical difference could be attributed to the errors of sintering behavior or the

measurement of relative permittivity.

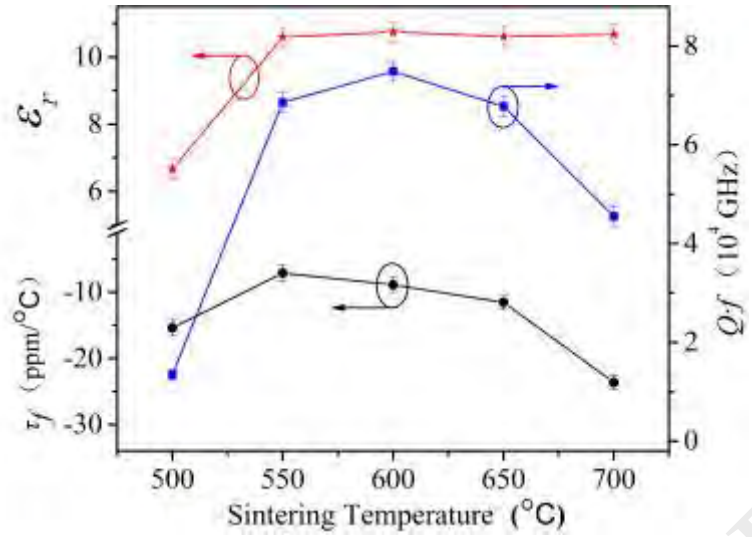

Fig. 4 Curves of ε_r, $Q{\cdot}f$, and τ_f values as a function of sintering temperatures for $Eu_2Zr_3(MoO_4)_9$ ceramics in the temperature range from 500 ℃ to 700 ℃.

The $Q{\cdot}f$ value of $Eu_2Zr_3(MoO_4)_9$ ceramics sintered at 500 ℃ to 700 ℃ was shown in Fig. 4. As can be seen in Table 1 and Fig. 4, along with the rise of sintering temperature, the density reached a maximum value when sample sintered at 600 ℃ and the quality factor reached the optimum value of 74,900 GHz. However, the quality factor began to decrease when sintering temperature became greater than 600 ℃, which could be attributed to the excessive sintering temperature. Fig. 4 also exhibited the tendency of τ_f values and it varied from -23.62 ppm/℃ to -7.09 ppm/℃. It is worth noting that the τ_f values were larger than that of $Ln_2Zr_3(MoO_4)_9$ (Ln=La, Sm, Nd) ceramics reported by Liu et al. [28, 29]. Besides, sample sintered at 550 ℃ could reach a near zero value of τ_f=-7.09 ppm/℃, which was better than the expectations.

There are two main factors influencing the microwave dielectric properties, the one is intrinsic factor and the other is extrinsic factor. The former include like crystal structure and lattice defects and the latter cover grain sizes, secondary phase, defect concentration, impurities, etc. [34, 35]. For the sake of exploring the relationship between microwave dielectric properties and the intrinsic factors, the complex chemical theory was used to calculate the bond ionicity, lattice energy, bond energy and the coefficient of thermal expansion and further characteristic the relationship. The P-V-L theory was used by Zhang et al. [36] to make the complex crystal decomposed into the sum of binary crystals as shown in Eq. (5), and make the further calculations afterwards.

$$\begin{aligned} Eu_2Zr_3(MoO_4)_9 \rightarrow\ & Eu_2 + Zr(1) + Zr(2)_2 + Mo(1)_6 + Mo(2)_3 \\ & + O(1)_6 + O(2)_6 + O(3)_6 + O(4)_6 + O(5)_6 + O(6)_6 \\ \rightarrow\ & Eu_{2/3}O(1)_3 + Eu_{2/3}O(2)_3 + Eu_{2/3}O(6)_3 \\ & + Zr(1)O(4)_3 + Zr(2)O(3)_3 + Zr(2)O(5)_3 \\ & + Mo(1)_{3/2}O(1)_3 + Mo(1)_{3/2}O(2)_3 + Mo(1)_{3/2}O(3)_3 \\ & + Mo(1)_{3/2}O(4)_3 + Mo(2)_{3/2}O(5)_3 + Mo(2)_{3/2}O(6)_3 \end{aligned} \quad (5)$$

Based on P-V-L theory, Batsanov et al. [37] figured out the relationship between bond ionicity and relative permittivity which was presented in Eq. (6), and it is obvious that the bond ionicity plays a significant role in effecting the relative permittivity. Thus, the bond with large ionicity made main contribution to the relative permittivity.

$$\varepsilon = \frac{n^2 - 1}{1 - f_i} + 1 \tag{6}$$

where n is the refractive index. The bond ionicity (f_i^{μ}) and bond covalency (f_c^{μ}) of an individual bond μ can be calculated as Eq. (S1)- (S5) [35, 36] and the results are listed in Table S3. In addition, the average bond ionicity of $f_{i(Eu-O)}$, $f_{i(Zr-O)}$ and $f_{i(Mo-O)}$ were 0.8501, 0.7914 and 0.7261, respectively. As a result, the sequence $f_{i(Eu-O)} > f_{i(Zr-O)} > f_{i(Mo-O)}$ proved that the bond ionicity of $f_{i(Eu-O)}$ played a dominate role in effecting relative permittivity.

Lattice energy is defined as the energy released when ions in the gas phase combine to form solid ionic crystals, so the higher the lattice energy, the stronger the ionic bonds. Therefore, lattice energy determines the stability of ionic crystals, which can explain and predict many physical and chemical properties of ionic crystals such as the quality factor. In addition, bond energy is a physical quantity that characterizes the strength of bonds, which can affect the quality factor as well. Lattice energy of an individual bond μ is defined by Eq. (S6)-(S9) [35, 36]. What's more, the bond energy can be obtained by the chemical bond and electronegativity theory reported by R.T. Sanderson [38-40]. And the calculated equations are shown in Eq. (S10)-(S14). The calculated average lattice energy and bond energy of each kind of bonds in $Eu_2Zr_3(MoO_4)_9$ ceramics were shown in Table S3. There was a sequence of lattice energy $U_{(Eu-O)} < U_{(Zr-O)} < U_{(Mo-O)}$ and bond energy $E_{(Eu-O)} < E_{(Zr-O)} < E_{(Mo-O)}$, which could prove that the lattice energy and bond energy of Mo-O bond played the predominant role in effecting quality factor.

τ_f value is a function of the temperature coefficient of the relative permittivity (τ_ε) and the thermal expansion coefficient (α) as shown in Eq. (7):

$$\tau_f = -\frac{\tau_\varepsilon}{2} - \alpha \tag{7}$$

As a result, τ_f value has a close relationship with the coefficient of thermal expansion. Based on the chemical bond theory and crystal parameter, the coefficient of thermal expansion α can be written as Eq. (S15). According to the results in Table S3, the value of α_{Mo-O} was negative and had a positive effect on τ_f value and the main negative factors to τ_f value were the coefficient of thermal expansion of Eu-O bond and Zr-O bond.

Microwave dielectric loss consists of two parts: intrinsic loss and extrinsic loss. The intrinsic loss was caused by lattice vibration acoustic mode and the extrinsic loss was by various defects of the ceramics. So far, it is impossible to accurately

and quantitatively analyze the contribution of the two loss modes to the quality factor. However, by means of the Kramers-Kronig (K-K) analysis, the contribution of lattice vibration to relative permittivity and dielectric loss could be obtained by extrapolating the infrared reflection spectrum fitting. A classical harmonic oscillator model written as Eq. (8) was used to analyse the IR spectra, and the relationship between the reflectivity and the complex relative permittivity was given by Fresnel's formulas shown in Eq. (9):

$$\varepsilon^*(\omega) = \varepsilon_\infty + \sum_{j=1}^{n} \frac{S_j^2}{\omega_j^2 - \omega^2 + j\omega\gamma_j} \tag{8}$$

$$R = \left| \frac{\sqrt{\varepsilon^*} - 1}{\sqrt{\varepsilon^*} + 1} \right|^2 \tag{9}$$

where $\varepsilon^*(\omega)$ was complex dielectric function, ε_∞ was relative permittivity caused by electronic polarization, R was the normal incidence reflectivity, n was the number of transverse phonon modes, S_j, ω_j and γ_j were plasma frequency, transverse frequency and damping factors of the J-th mode. Fig. 5 (a) presented the measured and fitted infrared reflectivity spectra for $Eu_2Zr_3(MoO_4)_9$ ceramics sintered at 600 ℃ and the fitted spectra matched well with the measured one. The fitted parameters of resonant modes in $Eu_2Zr_3(MoO_4)_9$ ceramics were listed in Table S4. Fig. 5 (b) plotted the the real and imaginary parts of the complex permittivity. The extrapolated permittivity value (13.267) in microwave region was slightly higher than the measured value (10.75) and the dielectric loss value was almost equal to the measured one, which indicated that the main polarization contribution for $Eu_2Zr_3(MoO_4)_9$ ceramics was the absorption of structural phonon oscillation at infrared region but not the defect phonon scattering [41].

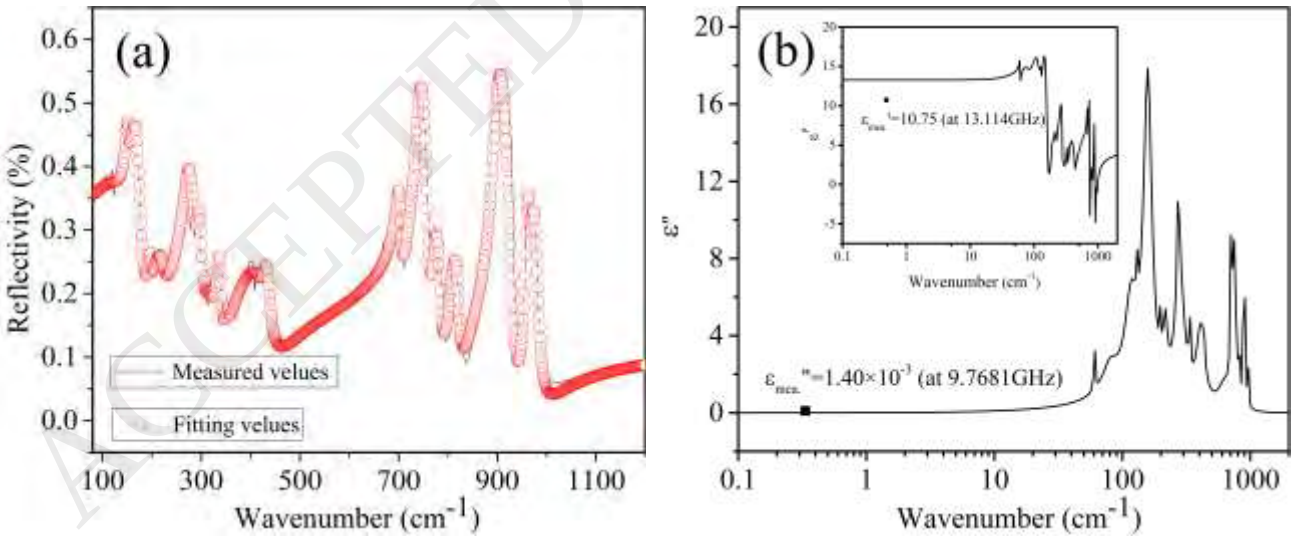

Fig. 5 (a) Measured and fitted infrared reflectivity spectra for $Eu_2Zr_3(MoO_4)_9$ ceramics sintered at 600 ℃ and (b) the real and imaginary parts of the complex permittivity for $Eu_2Zr_3(MoO_4)_9$ ceramics sintered at 600 ℃.

4. Conclusions

$Eu_2Zr_3(MoO_4)_9$ ceramics were synthesized by the traditional solid-state method. XRD pattern and Rietveld refinement

indicated that $Eu_2Zr_3(MoO_4)_9$ had a single phase structure belonging to a trigonal system with space group R-3c. SEM showed that ceramic sintered at 600 ℃ possessed dense and homogeneous grain. Based on the chemical bond theory, the ε_r value depended on the bond ionicity of Eu-O bond. The $Q{\cdot}f$ value was mainly affected by the lattice energy and bond energy of Mo-O bond. The coefficient of thermal expansion of Mo-O bond had a positive effect on τ_f value. In addition, Far infrared spectra indicated that the main polarization contribution for $Eu_2Zr_3(MoO_4)_9$ ceramics was the absorption of structural phonon oscillation at infrared region but not the defect phonon scattering. What's more, samples sintered at 600 ℃ for 4 h exhibited the best dielectric properties with ε_r=10.75, $Q{\cdot}f$=74,900 GHz and τ_f=-8.88 ppm/℃.

Acknowledgments

This work was supported by the National Natural Science Foundation (No. 51472108) and Project funded by China Postdoctoral Science Foundation (2017M612341). The authors are thankful to the help of Professor ZhenXing Yue and postdoctoral Jie Zhang on the measurement of microwave properties in Tsinghua University. The authors are also thankful to the administrators in IR beamline workstation of National Synchrotron Radiation Laboratory (NSRL) for the help in IR measurement.

Reference

[1] B. Liu, X.Q. Liu, X.M. Chen, Structural evolution and enhanced microwave dielectric properties in Sr^{2+}/Ti^{4+} co-substituted $SrNd_2Al_2O_7$ ceramics, J. Alloys. Compd. 758 (2018) 25-31.

[2] Z.F. Fu, J.L. Ma, P. Liu, Y. Liu, Novel temperature stable $Li_2Mg_3TiO_6$-$SrTiO_3$ composite ceramics with high Q for LTCC applications, Mater. Chem. Phys. 200 (2017) 264-269.

[3] G.Q. Zhang, J. Guo, X.F. Yuan, H. Wang, Ultra-low temperature sintering and microwave dielectric properties of a novel temperature stable $Na_2Mo_2O_7$-$Na_{0.5}Bi_{0.5}MoO_4$ ceramic, J. Eur. Ceram. Soc. 38 (2018) 813-816.

[4] Y. Wang, S.B. Zhang, T.L. Tang, W.S. Xia, L.W. Shi, Investigation on microwave dielectric properties of new low-loss $CoZrTa_2O_8$ ceramics, Mater. Lett. 231 (2018) 1-4.

[5] W.S. Xia, F.Y. Yang, G.Y. Zhang, K. Han, D.C. Guo, New low-dielectric-loss $NiZrNb_2O_8$ ceramics for microwave application, J. Alloys Compd. 656 (2016) 470-475.

[6] W.S. Xia, F. Jin, M. Wang, X. Wang, G.Y. Zhang, L.W. Shi, Effects of Al_2O_3 additive on sintering behavior and microwave dielectric properties of $ZnTa_2O_6$ ceramics, J. Mater. Sci.: Mater. Electron. 27 (2016) 1100-1104.

[7]. X.Q. Song, K. Du, X.Z. Zhang, J. Li, W.Z. Lu, X.C. Wang, et al., Crystal structure, phase composition and microwave dielectric properties of $Ca_3MSi_2O_9$ ceramics, J Alloys Compd. 750 (2018) 996-1002.

[8]. W.S. Xia, G.Y. Zhang, L.W. Shi, M.M. Zhang, Enhanced microwave dielectric properties of $ZnTa_2O_6$ ceramics with Sb^{5+} ion substitution, Mater. Lett. 124 (2014) 64-66.

[9]. Z.X. Fang, B. Tang, E.Z. Li, S.R. Zhang, High-Q microwave dielectric properties in the $Na_{0.5}Sm_{0.5}TiO_3$ + Cr_2O_3 ceramics by one synthetic process, J Alloys Compd. 705 (2017) 456-461.

[10] Y. Ohishi, Y. Miyauchi, H. Ohsato, K. Kakimoto, Controlled temperature coefficient of resonant frequency of Al_2O_3-TiO_2 ceramics by annealing treatment, Jpn. J. Appl. Phys. 43 (2004) 749-751.

[11] Y. Ohishi, Y. Miyauchi, K. Kakimoto, H. Ohsato, Microwave dielectric properties of Al_2O_3-TiO_2 improved by addition of ZnO, Ferroelectrics, 327 (2005) 27-31.

[12] H. Zheng, G.C.D. Gyorgyfalva, I.M. Reaney, Microstructure and microwave properties of $CaTiO_3$-$LaGaO_3$ solid solutions, J. Mater. Sci. 40 (2005) 5207-5214.

[13]. Y. Wang, L.Y. Zhang, S.B. Zhang, W.S. Xia, L.W. Shi, Sintering behavior and microwave dielectric properties of $MgZrTa_2O_8$ ceramics with fluoride addition, Mater. Lett. 219 (2018) 233–235.

[14]. W.S. Xia, L.Y. Zhang, Y. Wang, J.T. Zhang, R.R. Feng, L.W. Shi, Optimized sintering properties and temperature stability of $MgZrTa_2O_8$ ceramics with CuO addition for microwave application, J. Mater. Sci.: Mater. Electron. 28 (2017) 18437-18441.

[15] Y. Wang, R.Z. Zuo, A novel low-temperature fired microwave dielectric ceramic $BaMg_2V_2O_8$ with ultra-low loss, J. Eur.

Ceram. Soc. 36 (2016) 247-251.

[16] C.C. Li, H.C. Xiang, M.Y. Xu, J.B. Khaliq, J.Q. Chen, L. Fang, Low-firing and temperature stable microwave dielectric ceramics: $Ba_2LnV_3O_{11}$ (Ln=Nd, Sm), J. Am. Ceram. Soc. 101 (2018) 773-781.

[17] D. Chen, F. Luo, L. Gao, W.C. Zhou, D.M. Zhu, Dielectric and microwave absorption properties of divalent-doped $Na_3Zr_2Si_2PO_{12}$ ceramics, J. Eur. Ceram. Soc. 38 (2018) 4440-4445.

[18] K. Cheng, C.C. Li, H.C. Xiang, Y.H. Sun, L. Fang, $LiYGeO_4$: Novel low-permittivity microwave dielectric ceramics with intrinsic low sintering temperature, Mater. Lett. 228 (2018) 96-99.

[19] C.C. Li, H.C. Xiang, M.Y. Xu, Y. Tang, L. Fang, Li_2AGeO_4 (A=Zn, Mg): Two novel low-permittivity microwave dielectric ceramics with olivine structure, J. Eur. Ceram. Soc. 38 (2018) 1524-1528.

[20] X.F. Yuan, G.Q. Zhang, H. Wang, A novel solid solution $(K_{1-x}Na_x)_2Mo_2O_7$ ($0.0\leq x\leq 0.3$) ceramics with ultra-low sintering temperatures, J. Eur. Ceram. Soc. 38 (2018) 4967-4971.

[21] J.Q. Chen, Y. Tang, H.C. Xiang, L. Fang, C.C. Li, Microwave dielectric properties and infrared reflectivity spectra analysis of two novel low-firing $AgCa_2B_2V_3O_{12}$ (B=Mg, Zn) ceramics with garnet structure, J. Eur. Ceram. Soc. 38 (2018) 4670-4676.

[22] P. Zhang, S.X. Wu, M. Xiao, The microwave dielectric properties and crystal structure of low temperature sintering $LiNiPO_4$ ceramics, J. Eur. Ceram. Soc. 38 (2018) 4433-4439.

[23] H. Yang, B. Tang, Z.X. Fang, A new low-firing and high-Q microwave dielectric ceramic $Li_9Zr_3NbO_{13}$, J. Am. Chem. Soc. 101 (2018) 2202-2207.

[24] W.Q. Liu, R.Z. Zuo, A novel Li_2TiO_3-Li_2CeO_3 ceramic composite with excellent microwave dielectric properties for low-temperature cofired ceramic applications, J. Eur. Ceram. Soc. 38 (2018) 119-123.

[25] L.X. Pang, D. Zhou, W.G. Liu, Low-temperature sintering and microwave dielectric properties of $CaMoO_4$-based temperature stable LTCC material, J. Am. Ceram. Soc. 97 (2014) 2032-2034.

[26] L.X. Pang, G.B. Sun, D. Zhou, $Ln_2Mo_3O_{12}$ (Ln=La, Nd): A novel group of low loss microwave dielectric ceramics with low sintering temperature, Mater. Lett. 65 (2011) 164-166.

[27] G.Q. Zhang, J. Guo, H. Wang, Ultra-low temperature sintering microwave dielectric ceramics based on Ag_2O-MoO_3 binary system, J. Am. Ceram. Soc. 100 (2017) 2604-2611.

[28] W.Q. Liu, R.Z. Zuo, Low temperature fired $Ln_2Zr_3(MoO_4)_9$ (Ln=Sm, Nd) microwave dielectric ceramics, Ceram. Int. 43 (2017) 17229-17232.

[29] W.Q. Liu, R.Z. Zuo, A novel low-temperature firable $La_2Zr_3(MoO_4)_9$ microwave dielectric ceramic, J. Eur. Ceram. Soc. 38 (2018) 339-342.

[30] B.W. Hakki, P.D. Coleman, A dielectric resonator method of measuring inductive capacities in the millimeter range, IRE Trans. Microw. Theory Tech. 8 (1960) 402-410.

[31] W.E. Courtney, Analysis and evaluation of a method of measuring the complex permittivity and permeability microwave Insulators, IEEE Trans. Microw. Theory Tech. 18 (1970) 476-485.

[32] R.D. Shannon, Dielectric polarizabilities of ions in oxides and fluorides, J. Appl. Phys. 73 (1993) 348-366.

[33] G.K. Choi, J.R. Kim, S.H. Yoon, K.S. Hong, Microwave dielectric properties of scheelite (A=Ca, Sr, Ba) and wolframite (A=Mg, Zn, Mn) $AMoO_4$ compounds, J. Eur. Ceram. Soc. 27 (2007) 3063-3067.

[34] Z. Fu, J. Ma, P. Liu, B.C. Guo, X.M. Chen, Microwave dielectric properties of low-fired Li_2MnO_3 ceramics co-doped with LiF-TiO_2, Ceram. Int. 42 (2016) 6005-6009.

[35] W.S. Xia, L.Y. Zhang, Y. Wang, S.E. Jin, Y.P. Xu, Z.W. Zuo, Extrinsic effects on microwave dielectric properties of high-Q $MgZrTa_2O_8$ ceramics, J Mater Sci: Mater Electron. 27 (2016) 11325-11330.

[36] Z.J. Wu, Q.B. Meng, S.Y. Zhang, Semi empirical study on the valences of Cu and bond covalency in $Y_{1-x}Ca_xBa_2Cu_3O_{6+y}$, Phys. Rev. B 58 (1998) 958-962.

[37] S.S. Batsanov, Dielectric methods of studying the chemical bond and the concept of electronegativity, Russ. Chem. Rev. 51 (1982) 684-697.

[38] R.T. Sanderson, Multiple and single bond energies in inorganic molecules, Inorg. Nucl. Chem. 30 (1968) 375-393.

[39] R.T. Sanderson, Chemical bonds, bond energy, Academic press, New York, 1971.

[40] R.T. Sanderson, Electronegativity and bond energy, J. Am. Chem. Soc. 105 (1983) 2259-2261.

[41] L.X. Pang, D. Zhou, W.G. Liu, Z.M. Qi, Z.X. Yue, Crystal structure and microwave dielectric behaviors of scheelite structured (1-x)$BiVO_4$-x$La_{2/3}MoO_4$ ($0.0 \leq x \leq 1.0$) ceramics with ultra-low sintering temperature, J. Eur. Ceram. Soc. 38 (2018) 1535-1540.

Figures captions

Fig. 1 X-Ray diffraction patterns of calcined powders sintered at 600 ℃ for 2h and $Eu_2Zr_3(MoO_4)_9$ ceramics sintered at 600 ℃-700 ℃ for 4h.

Fig. 2 Schematic representation of the crystal structure for $Eu_2Zr_3(MoO_4)_9$ ceramics.

Fig. 3 SEM micrographs of $Eu_2Zr_3(MoO_4)_9$ ceramics sintered at different temperatures for 4 h (a-c corresponding to 600 ℃-700 ℃).

Fig. 4 Curves of ε_r, $Q{\cdot}f$, and τ_f values as a function of sintering temperatures for $Eu_2Zr_3(MoO_4)_9$ ceramics in the temperature range from 500 ℃ to 700 ℃.

Fig. 5 (a) Measured and fitted infrared reflectivity spectra for $Eu_2Zr_3(MoO_4)_9$ ceramics sintered at 600 ℃ and (b) the real and imaginary parts of the complex permittivity for $Eu_2Zr_3(MoO_4)_9$ ceramics sintered at 600 ℃.